JOURNAL OF AIRCRAFT
Vol. 47, No. 4, July–August 2010

Rapid Estimation of Impaired-Aircraft Aerodynamic Parameters

Jinwhan Kim,* Karthik Palaniappan,† and P. K. Menon‡
Optimal Synthesis, Inc., Los Altos, California 94022

DOI: 10.2514/1.46914

An estimation of aerodynamic models of impaired aircraft using an innovative differential vortex-lattice method tightly coupled with extended Kalman filters is discussed. The proposed approach significantly reduces the order of the estimation problem by exploiting the prior knowledge about the undamaged aircraft and the detected information on the approximate location and extent of damage. Three different extended Kalman filter formulations are developed and their comparative analyses are performed through numerical simulations. Algorithms given in this paper can be used as the basis for online derivation of an aircraft performance model, which can then form the basis for designing safe landing guidance laws for damaged aircraft.

Nomenclature

A_G = aircraft geometry
$C_{m,n}$ = normal influence coefficient for the nth horseshoe-vortex effect at the mth panel
D = drag
$D_{m,n}$ = nonlinear function that relates the pressure difference at the mth panel to the nth horseshoe-vortex effect
$\mathbf{F}$ = system dynamics Jacobian matrix
$\mathbf{f}$ = continuous-time system dynamics function
g = gravitational acceleration
$\mathbf{H}_k$ = measurement Jacobian matrix
$\mathbf{h}_k$ = discrete-time measurement function
L = lift
M = mass
$\mathbf{P}$ = state estimate error covariance matrix
$\mathbf{Q}$ = process noise covariance matrix
$\mathbf{R}_k$ = measurement noise covariance matrix
S = side force
T = maximum thrust
V = velocity
V_m = normal velocity at the control point of the mth panel
V_∞ = airspeed
$\mathbf{v}_k$ = measurement noise vector
$\mathbf{w}$ = process noise vector
x = north position
$\mathbf{x}$ = continuous-time system state vector
y = east position
z = altitude
$\mathbf{z}_k$ = discrete-time measurement vector
α = angle of attack
α_m = angle of attack at the mth control point
β = angle of sideslip
Γ = circulation-strength distribution
Γ_m = circulation strength at the mth control point
γ = flight-path angle
δp_m = pressure difference between the lower and upper surfaces at the control point of the mth panel
$\delta\Gamma$ = circulation-strength difference between impaired and unimpaired values
ε_m = local wing twist at the mth control point
ζ = leakage constant (or fictitious damping coefficient)
η = thrust throttle level
ρ = air density
ϕ = bank angle
χ = heading angle

Presented as Paper 2009-6087 at the AIAA Guidance, Navigation, and Control Conference, Chicago, IL, 10–13 August 2009; received 28 August 2009; revision received 25 January 2010; accepted for publication 1 February 2010.

*Research Scientist, 95 First Street, Suite 240. Senor Member AIAA.
†Senior Researcher; currently General Motors India Science Laboratory. Member AIAA.
‡Chief Scientist, 95 First Street, Suite 240. Fellow AIAA.

I. Introduction

MODERN flight control systems have enabled safer operation of civil and military aircraft by making the machines more compatible with the human pilots. This has been achieved through advances in automatic control theory, together with modern sensors and computing hardware. Design methods have now reached such an advanced level of sophistication that systematic methods are available for synthesizing flight control systems of extremely complex aircraft. The next frontier in this discipline is that of creating flight control systems that can maintain safe flight after significant damage to the aircraft and allow it to land with no loss of life or property. This sentiment is succinctly expressed in the stated goal of NASA's Integrated Resilient Aircraft Control program.

Over the past decades, several well-documented examples of aircraft survival after extreme airframe damage have become available. These have included both high-performance military aircraft and large passenger jets. In each case, the pilot skill was the central factor in enabling positive outcomes. The objective of damage-adaptive flight control systems research is to incorporate sufficient intelligence into next-generation flight control systems so that the pilots have adequate resources available onboard to facilitate a favorable outcome after damage.

Methods for adaptive control of damaged aircraft are being investigated at NASA and other aerospace research laboratories in the United States [1–3]. The focus of these research efforts is on maintaining closed-loop stability of the autopilot after damage. Assuming that the aircraft remains controllable at its current flight conditions, it is important to be able to predict its performance at other flight conditions in order to derive the maneuver constraints to be enforced for safe transition into the landing configuration.

The objective of the research discussed in this paper is to develop estimation schemes for rapidly extracting the aerodynamic parameters of impaired aircraft in order to enable the assessment of aircraft performance. The performance data of interest include flight-envelope boundaries and maneuver limits. These data can form the basis for the design of safe landing guidance laws.

Several innovative concepts are advanced in this paper. First, a rapid approach for deriving aerodynamic models of impaired aircraft, termed the differential vortex-lattice method (DVLM), is developed. This approach recasts the well-known vortex-lattice method (VLM) [4,5] to reduce the dimension of the aerodynamic problem. The DVLM formulation exploits prior knowledge about the airframe to create a low-order computational methodology for relating the changes in the vehicle geometry due to damage to its aerodynamic parameters. This low-order method can be implemented in real-time onboard for the aircraft to provide estimates of the aerodynamic parameters.

Second, the extended Kalman filtering (EKF) approach [6–8] is employed for online estimation of impaired-aircraft parameters based on the DVLM. The design of maneuvers for enhancing the observability of the impaired-aircraft model parameters is also discussed. The model parameters derived from the estimator can be used for computing flight-envelope and maneuver limits. These can then be used in the synthesis of safe guidance laws for landing the aircraft.

Unlike the airframe stabilization problem, the guidance task is almost entirely based on predictive information about the aircraft dynamics. For example, landing guidance requires the aircraft to slow down to the approach speeds while descending to the correct altitude at a specified heading. Since impaired aircraft may have a high drag and lower stall angle of attack, the aircraft energy has to be carefully managed to ensure that adequate lift is maintained until flare altitude and touchdown. This will require energy-conservative maneuvers and descent strategies. Since an impaired aircraft may not be able to employ all of its high-lift devices, its speed must be carefully managed to avoid premature loss of lift. These factors make it important to derive a reasonably accurate performance model of the aircraft for the design of a viable guidance system. It may be noted that although most inner-loop flight control systems operate well within the limits of controllability most of the time, the guidance task often involves operating near the edges of the operational envelope.

This motivates the use of the indirect adaptive control framework [9] for the guidance problem, wherein an estimation procedure is used to find the parameters of the model, which then forms the basis for the design of guidance commands. Because of the use of predictive information available in the estimated model, this problem must be formulated carefully to ensure that the model closely approximates the expected dynamics of the impaired aircraft. This is because of the fact that due to their dependence on predictive information, guidance systems are much more susceptible to modeling uncertainties.

The present research is motivated by the desirability of relating the damaged aircraft geometry with its flight dynamics. Central premises involved in the research are that the inner-loop flight control system allows the continued flight of the aircraft, the onboard sensors such as electronic cameras integrated with the airframe can provide information about the location of the damage, and the well-known vortex-lattice method can provide sufficiently accurate aerodynamic characterization of the damaged aircraft.

Section II presents the equations of motion and the associated filter formulation. The DVLM is described in Sec. III. The DVLM-based nonlinear filter formulations with various parameterization methods are given in Sec. II. The performance validation based on numerical simulations is presented in Sec. V, and the conclusions from the present research are given in Sec. VI.

II. Equations of Motion and Filter Formulation

The proposed approach for online estimation of impaired-aircraft performance uses a nonlinear online estimation algorithm in conjunction with the DVLM. This paper focuses on investigating the feasibility of the proposed estimation algorithm. A 3-D point-mass model is used for describing the motion of aircraft by assuming that the kinematic states have been stabilized by the inner-loop controller. Since the system dynamics are nonlinear, an EKF algorithm is used in the filter formulation proposed in this research.

A. Point-Mass Aircraft Dynamics

The 3-D point-mass dynamics of an aircraft are used to describe the motion of aircraft in 3-D configuration space. This model assumes that the control variables continuously maintain the aircraft moment equilibrium, such that the aircraft can follow commanded angle of attack, angle of side slip, and/or bank angle. Based on the coordinate system shown in Fig. 1, the equations of motion can be expressed in the form

$$\dot{\mathbf{x}} = \begin{bmatrix} \dot{V} \\ \dot{\gamma} \\ \dot{\chi} \\ \dot{x} \\ \dot{y} \\ \dot{z} \end{bmatrix} = \begin{bmatrix} (\eta T - D)/M - g\sin\gamma \\ (L\cos\phi - S\sin\phi)/(MV) - g\cos\gamma/V \\ (L\sin\phi - S\cos\phi)/(MV\cos\gamma) \\ V\cos\gamma\sin\chi \\ V\cos\gamma\cos\chi \\ V\sin\gamma \end{bmatrix} \tag{1}$$

In Eq. (1), the maximum thrust T is assumed to be constant, and the actual thrust is assumed to vary linearly with respect to the throttle setting η.

B. Computing the Forces on an Impaired Aircraft Using DVLM

Under normal operating conditions, the lift, drag, and side force in Eq. (1) can be expressed as functions of aircraft geometry and aerodynamic parameters such as dynamic pressure, angle of attack, and angle of sideslip.

If physical damage occurs to the airframe, both the aircraft geometry and the aerodynamic parameters change, and consequently the original relationships are no longer valid in describing the aerodynamic forces and the resulting motions. The VLM is capable of describing the aerodynamic forces based on the airframe geometry, and the distribution of circulation over discretized panels defining the geometric airframe can be calculated and integrated into forces at the given flight conditions: that is,

$$\begin{aligned} L &= L(\rho, \Gamma, A_G, V_\infty, \alpha, \beta) \\ D &= D(\rho, \Gamma, A_G, V_\infty, \alpha, \beta) \\ S &= S(\rho, \Gamma, A_G, V_\infty, \alpha, \beta) \end{aligned} \tag{2}$$

The aerodynamic forces are dependent on air density, circulation-strength distributions, aircraft geometry, airspeed, angle of attack, and angle of sideslip. Note that the circulation components are also functions of the aircraft geometry and the flight conditions. In the conventional VLM, the dimension of Γ is equal to the number of panels approximating the airframe, which is normally a large number. Designing online recursive estimators based on the VLM is unrealistic due to its high dimension.

The DVLM proposed in this paper allows the calculation of the forces on the impaired aircraft using differential circulation-strength components in the vicinity of the impaired section, involving a much smaller set of circulation strengths when compared with the conventional VLM approach. The associated reduction in the dimension allows the DVLM to be used as the basis for the derivation of recursive estimators.

C. EKF-Based State-Parameter Estimation

The state-parameter estimation problem is often called the dual-estimation problem because it requires the simultaneous estimation of the system states and the unknown parameters. In general, these

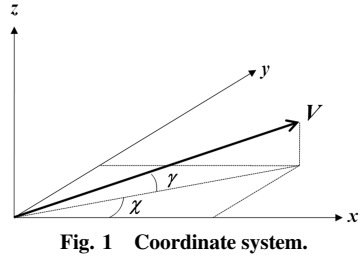

Fig. 1 Coordinate system.

problems involve system nonlinearities and nonlinear coupling between the states and the parameters. The EKF is most widely and commonly used for the formulation of nonlinear dual estimators. The implementation procedure of the EKF proceeds as follows:

For a given nonlinear system with unknown system parameters,

$$\dot{\mathbf{x}} = \mathbf{f}(\mathbf{x}, \boldsymbol{\theta}) + \mathbf{w} \tag{3}$$

where $\mathbf{x}$ is the system state vector, $\boldsymbol{\theta}$ is the parameter vector to be estimated, and $\mathbf{f}(\cdot)$ is the nonlinear function of states and parameters. The process noise $\mathbf{w}$ is assumed to be Gaussian in the EKF development.

The dynamic model of the parameters $\boldsymbol{\theta}$ is chosen based on any prior knowledge about its temporal behavior. The simplest model assumption is that of $\boldsymbol{\theta}$ being piecewise-constant functions.

The augmented system dynamics can then be written as

$$\dot{\mathbf{x}}^{\mathbf{a}} = \begin{bmatrix} \dot{\mathbf{x}} \\ \dot{\boldsymbol{\theta}} \end{bmatrix} = \begin{bmatrix} \mathbf{f}(\mathbf{x}, \boldsymbol{\theta}) \\ \mathbf{0} \end{bmatrix} + \mathbf{w}^{\mathbf{a}} \tag{4}$$

Here, $\mathbf{x}^{\mathbf{a}}$ is the augmented system state vector. Although $\boldsymbol{\theta}$ is assumed to be piecewise-constant, this model allows moderate time variations in the parameters through the augmented process noise vector $\mathbf{w}^{\mathbf{a}}$.

The remaining filter design procedure is the same as that of the standard EKF implementation procedure. Table 1 provides a summary of the continuous-discrete EKF based on the first-order Euler integration method employed in the present study.

Aircraft position, velocity, and acceleration measurements are assumed to be available for the present state-parameter estimation process: namely,

$$\mathbf{z}_k = [V \quad \gamma \quad \chi \quad x \quad y \quad z \quad \dot{V} \quad \dot{\gamma} \quad \dot{\chi}]^T_{t=t_k} + \mathbf{v}_k \tag{5}$$

III. Differential Vortex-Lattice Method

A. Equations of Motion

The VLM is based on inviscid, incompressible, steady, and irrotational flow assumptions and has proven to be highly effective for determining aerodynamic characteristics of the complete aircraft configurations [10–12]. Once the aerodynamic model has been determined, it can be used to predict the performance characteristics of the aircraft.

The first stage in the implementation of the VLM is the discretization of the vehicle geometry into vortex panels, as shown in Fig. 2. The entire wing surface is divided into a number of vortex panels laid out in a latticelike structure. A horseshoe vortex is placed at the quarter-chord location of each panel. In the classical implementation of the vortex-lattice method, the trailing vortices are assumed to extend to infinity. The wake is assumed to be flat, and the control points are assumed to lie at the three-quarter point of each panel.

The normal velocity at the control point of the mth panel due to the horseshoe vortex at the nth panel is given by

$$V_m = C_{m,n}\Gamma_n \tag{6}$$

where $C_{m,n}$ is the influence coefficient for the nth horseshoe-vortex effect at the mth panel in the normal direction. The parameter $C_{m,n}$ depends on the geometry of the wing [5] and can be precomputed and stored onboard. Consequently, the normal velocity at the mth control point due to all the vortices on the wing surface can be written as

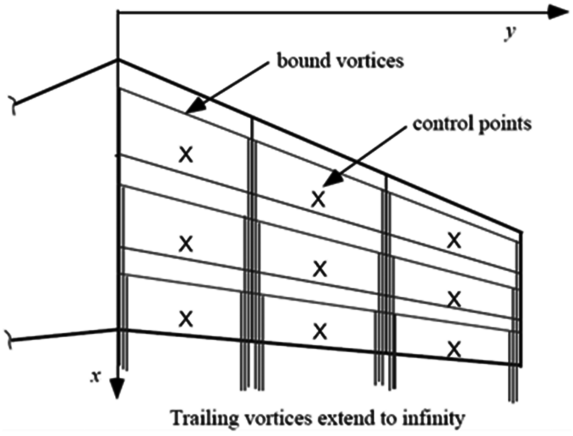

Fig. 2 Discretization of a wing surface into vortex panels.

$$V_m = \sum_{n=1}^{N} C_{m,n}\Gamma_n \tag{7}$$

The standard boundary condition imposed at any one of these control points ensures that the total normal velocity at any one of these control points is zero (i.e., *no-penetration* boundary condition). This is enforced as follows:

$$V_m + V_\infty \sin(\alpha_m + \varepsilon_m) = \sum_{n=1}^{N} C_{m,n}\Gamma_n + V_\infty \sin(\alpha_m + \varepsilon_m) = 0 \tag{8}$$

Here, α_m and ε_m are the angle of attack and the local wing twist at the mth control point. The above equation can then be written in matrix form as

$$\begin{bmatrix} C_{1,1} & \cdots & C_{1,N} \\ \vdots & \ddots & \vdots \\ C_{N,1} & \cdots & C_{N,N} \end{bmatrix} \begin{bmatrix} \Gamma_1 \\ \vdots \\ \Gamma_N \end{bmatrix} = \begin{bmatrix} -V_\infty \sin(a_1 + \varepsilon_1) \\ \vdots \\ -V_\infty \sin(a_N + \varepsilon_N) \end{bmatrix} \rightarrow \mathbf{C}\Gamma = \mathbf{b} \tag{9}$$

In Eq. (9), the square matrix on the left-hand side, $\mathbf{C}$, depends only on the geometry of the wing. The vector of the boundary condition on the right-hand side, $\mathbf{b}$, depends on the freestream velocity V_∞, the local angle of attack α_m, and the local wing twist ε_m. The vector of circulation strengths of the horseshoe vortices Γ can be obtained by solving the above matrix equation.

Once the circulation-strength vector is known, the pressure difference between the lower and upper surfaces at the locations of the mth control points can be calculated as

Table 1 Continuous-discrete extended Kalman filter [6]

	Equations	Definitions
System model	$\dot{\mathbf{x}} = \mathbf{f}(\mathbf{x}) + \mathbf{w}$	$\mathbf{w} \sim N(\mathbf{0}, \mathbf{Q})$
Measurement model	$\mathbf{z}_k = \mathbf{h}_k(\mathbf{x}_k) + \mathbf{v}_k$	$\mathbf{v}_k \sim N(\mathbf{0}, \mathbf{R}_k)$
Time propagation	$\dot{\hat{\mathbf{x}}} = \mathbf{f}(\hat{\mathbf{x}}) \rightarrow \hat{\mathbf{x}}_k^- = \hat{\mathbf{x}}_{k-1}^+ + (t_k - t_{k-1})\dot{\hat{\mathbf{x}}}$ $\dot{\mathbf{P}} = \mathbf{FP} + \mathbf{PF}^{\mathbf{T}} + \mathbf{Q} \rightarrow \mathbf{P}_k^- = \mathbf{P}_{k-1}^+ + (t_k - t_{k-1})\dot{\mathbf{P}}$	$\mathbf{F} = [\frac{\partial \mathbf{f}}{\partial \mathbf{x}}]_{\mathbf{x}=\hat{\mathbf{x}}}$
Measurement update	$\hat{\mathbf{x}}_k^+ = \hat{\mathbf{x}}_k^- + \mathbf{L}_k[\mathbf{z}_k - \mathbf{h}_k(\mathbf{x}_k)]$ $\mathbf{P}_k^+ = (\mathbf{I} - \mathbf{L}_k\mathbf{H}_k)\mathbf{P}_k^-$	$\mathbf{H}_k = [\frac{\partial \mathbf{h}_k}{\partial \mathbf{x}}]_{\mathbf{x}=\hat{\mathbf{x}}_k^-}$ $\mathbf{L}_k = \mathbf{P}_k^-\mathbf{H}_k^{\mathbf{T}}(\mathbf{H}_k\mathbf{P}_k^-\mathbf{H}_k^{\mathbf{T}} + \mathbf{R}_k)^{-1}$

$$\delta p_m = (p_L - p_U)_m = \sum_{n=1}^{N} D_{m,n}(\Gamma_n) \tag{10}$$

where $D_{m,n}$ is a nonlinear function that relates the pressure difference at the mth panel to the effect of the nth horseshoe vortex. The nonlinear function $D_{m,n}$ also depends on the wing geometry [5].

The resulting aerodynamic forces along the x, y, and z axes are then given, respectively, by

$$F_x = \sum_{n=1}^{N} \delta p_n \, \mathrm{d}A_{n,x} \quad F_y = \sum_{n=1}^{N} \delta p_n \, \mathrm{d}A_{n,y} \quad F_z = \sum_{n=1}^{N} \delta p_n \, \mathrm{d}A_{n,z} \tag{11}$$

B. Differential Vortex-Lattice Method Formulation

The DVLM advanced in the present research significantly reduces the dimension of the problem by exploiting the knowledge about the circulation over the aircraft structure before the damage. The DVLM problem is formulated in terms of the changes in the circulation on the panels in the neighborhood of the damage.

Let the circulation distribution over an unimpaired wing be given by

$$\mathbf{C}\,\Gamma = \mathbf{b} \tag{12}$$

Here, Γ is the array containing the circulation strengths in the different panels, arranged in some predetermined manner. The element $C_{i,j}$ of $\mathbf{C}$ represents the aerodynamic influence of the jth panel on the ith panel. It should be noted that

$$C_{i,j} \propto \frac{1}{r_{i,j}^2} \tag{13}$$

where $r_{i,j}$ is the distance between the ith and jth panels. When a portion of the airframe is impaired, the circulation strength at that location can be assumed to go to zero. At this point, it is useful to note that the influence of the impaired panels is felt strongly only at the neighboring panels and can be regarded as insignificant if the panels are sufficiently far away.

It is important to get a quantitative idea of the decay of the influence of the impaired panel. Consider a wing of span s, divided into n panels of the same size, spanwise. For the purposes of illustration, consider only one chordwise panel. The size of each panel is then given by s/N. The distance between the control point of a panel and its periphery, where the bound vortex is assumed to be, is given by half this distance $s/(2N)$. The influence on a panel due to its own circulation is then given by

$$C_{i,i} \propto \frac{4N^2}{s^2} \tag{14}$$

The influence on a panel due to another panel, n panels away, is given by

$$C_{i,i+n} \propto \frac{N^2}{n^2 s^2} \tag{15}$$

The ratio of the influences is then given by

$$\frac{C_{i,i+n}}{C_{i,i}} = \frac{1}{4n^2} \tag{16}$$

It can be seen that the above equation is independent of the span s and the total number of panels chosen N. If n is 2, the ratio of influences is 6.25%, and if n is 3, it is 2.77%. Thus, for example, if an error of 3% can be tolerated, it is sufficient to study flow over three panels adjacent to the impaired area on all sides. This has the advantage of reducing the area of computation of circulation strengths to three neighboring panels. Hence, the values of the vortex-strength distribution for a damaged case can sufficiently be approximated as the values for the corresponding undamaged case, except at locations three panels away in each direction from the location of damage.

For the proposed DVLM formulation, all of the surface panels are divided into three groups:

1) Panel group 1 contains undamaged panels that are some distance away from the damaged section, where the effect of damage can be assumed to be negligible or insignificant.

2) Panel group 2 contains damaged panels which have been taken off from the airframe. These panels produce no aerodynamic force at all.

3) Panel group 3 contains undamaged panels that are in the close neighborhood of the damaged area. The effect of the damage can be felt strongly and clearly over these panels.

Then the equation for circulation for an impaired airframe can be expressed by the following partitioned matrix equation:

$$\begin{bmatrix} \mathbf{A_{1,1}} & \mathbf{A_{1,2}} & \mathbf{A_{1,3}} \\ \mathbf{A_{2,1}} & \mathbf{A_{2,2}} & \mathbf{A_{2,3}} \\ \mathbf{A_{3,1}} & \mathbf{A_{3,2}} & \mathbf{A_{3,3}} \end{bmatrix} \begin{bmatrix} \Gamma_1 + \delta\Gamma_1 \\ \Gamma_2 + \delta\Gamma_2 \\ \Gamma_3 + \delta\Gamma_3 \end{bmatrix} = \begin{bmatrix} \mathbf{b_1} \\ \mathbf{b_2} \\ \mathbf{b_3} \end{bmatrix} \tag{17}$$

Here, the subscript represents the panel group number, $\Gamma_\mathbf{i}$ is the circulation-strength vector for the unimpaired airframe, and $\delta\Gamma_\mathbf{i}$ represents the circulation-strength difference between impaired and unimpaired values for each group of panels.

The first panel group is little affected by damage and thus $\delta\Gamma_\mathbf{1}$ can be assumed to be close to zero. The second panel group does not contribute to lift and thus can be ignored. The third group is the panels in the vicinity of the damaged section. The circulation strengths over these panels are likely to be significantly affected by the damage, and thus the differential vector $\delta\Gamma_\mathbf{3}$ is expected to have larger nonzero values. Then Eq. (17) can be approximated as

$$\begin{bmatrix} \mathbf{A_{1,1}} & \mathbf{A_{1,3}} \\ \mathbf{A_{3,1}} & \mathbf{A_{3,3}} \end{bmatrix} \begin{bmatrix} \Gamma_\mathbf{1} \\ \Gamma_3 + \delta\Gamma_3 \end{bmatrix} = \begin{bmatrix} \mathbf{b_1} \\ \mathbf{b_3} \end{bmatrix} \tag{18}$$

and the expression for $\delta\Gamma_\mathbf{3}$ becomes

$$\delta\,\Gamma_\mathbf{3} = \mathbf{A_{3,3}^{-1}}(\mathbf{b_3} - \mathbf{A_{3,1}}\Gamma_\mathbf{1}) - \Gamma_3 \tag{19}$$

This is the fundamental hypothesis of the DVLM. The process of formulating the differential circulation is illustrated in Fig. 3.

The corrected circulation vector can be used to evaluate the pressure distribution on the impaired airframe. The pressure distribution can then be integrated to produce aerodynamic forces. The aerodynamic forces can then be normalized with respect to dynamic pressure and reference area to yield drag, lift, and side-force coefficients. The DVLM computation procedure is summarized in Fig. 4.

C. Analysis of Computational Complexity

The differential scheme described in the previous subsection enables transforming the original problem with a large number of unknown circulation strengths into a reduced problem involving a much smaller number of unknowns. Table 2 compares the order of computation operations of the standard VLM and DVLM.

In terms of computation complexity, the most expensive operation of the VLM algorithm is the matrix inversion whose complexity is $\mathbf{O}(N^3)$, where N is the dimension of the circulation-strength vector. For the conventional VLM, N is the total number of surface panels over the entire airframe (i.e., $N = n$). However, for the proposed DVLM approach, it is the number of panels in the vicinity of the damaged section (i.e., $N = k$), which leads to a significant computational savings, since $n \gg k$.

IV. DVLM-Based EKF Formulations

This section will discuss two DVLM-based EKF formulations with different sets of parameter states.

In formulation 1, circulation-strength estimation, circulation-strength distributions are introduced as the system parameters to be estimated. Two variations of this estimation problem will be discussed.

In formulation 2, parameterized-damage estimation, the extent of damage is directly estimated by an appropriate parameterization of the damage.

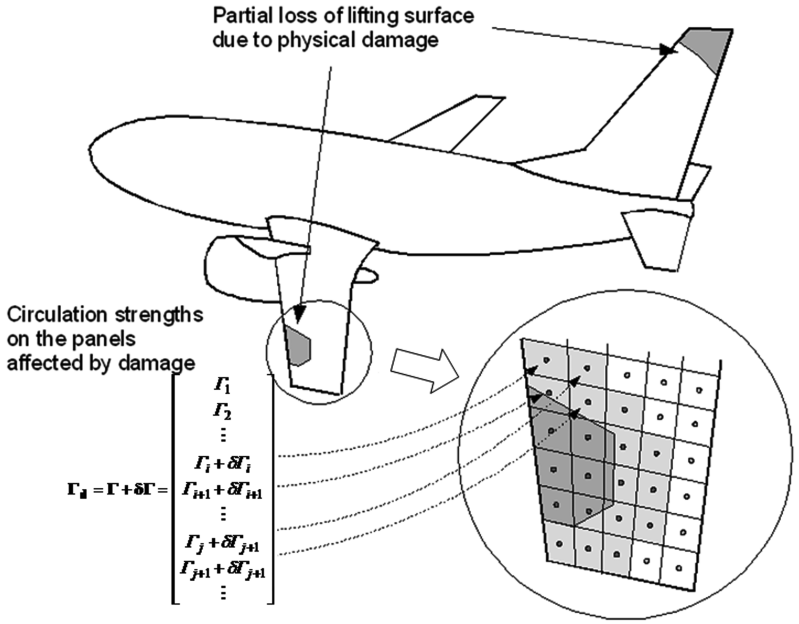

Fig. 3 Modeling airframe damage using differential vortex-lattice method.

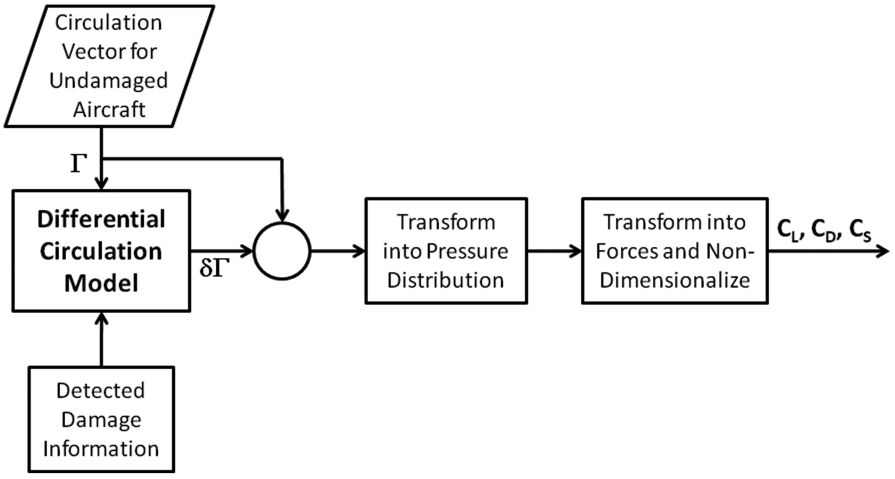

Fig. 4 Summary of the differential vortex-lattice method.

Details of these two approaches are presented in the following subsections.

A. Formulation 1: Direct Estimation of the Differential Circulation Vector

The filter is initialized with the precomputed unimpaired-aircraft circulation-strength vector and the measured state vector. Given the aircraft position, velocity, and acceleration vectors derived from the Global Positioning System and inertial navigation system (GPS/INS), and air data sensors onboard, the EKF will generate estimates of the differential circulation vector and the resulting aerodynamic coefficients. The overall block-diagram structure together with a potential closed-loop guidance system are given in Fig. 5.

In addition to the estimator block, the above block diagram includes the guidance block for computing a safe landing trajectory based on the estimated flight envelope for the damaged airframe, the point-mass dynamics block that approximates the actual dynamic of the aircraft, and the sensor block that provides motion information to the estimator.

The present research focuses on designing the estimator block assuming that motion measurements and approximate damage information are provided by onboard sensors. The impaired-aircraft guidance problem is currently being developed. The augmented system dynamics for the state-parameter estimation problem can be written as follows:

$$\dot{\mathbf{x}}^{\mathbf{a}} = \begin{bmatrix} \dot{V} \\ \dot{\gamma} \\ \dot{\chi} \\ \dot{x} \\ \dot{y} \\ \dot{z} \\ \delta\dot{\Gamma}_1 \\ \delta\dot{\Gamma}_2 \\ \vdots \\ \delta\dot{\Gamma}_m \end{bmatrix} = \begin{bmatrix} (\eta T - D)/M - g\sin\gamma \\ (L\cos\varphi - S\sin\varphi)/(MV) - g\cos\gamma/V \\ (L\sin\varphi - S\cos\varphi)/(MV\cos\gamma) \\ V\cos\gamma\sin\chi \\ V\cos\gamma\cos\chi \\ V\sin\gamma \\ -\zeta_1\delta\Gamma_1 \\ -\zeta_2\delta\Gamma_2 \\ \vdots \\ -\zeta_m\delta\Gamma_m \end{bmatrix} + \mathbf{w}^{\mathbf{a}} \quad (20)$$

Here, $\mathbf{w}^a$ is the augmented process noise vector. The associated Jacobian matrix for the augmented system dynamics, $\mathbf{F}^{\mathbf{a}}$, can be expressed as

Table 2 Computational complexity comparison between the standard VLM and DLVM[a]

Operation	Standard VLM	DMVL
Matrix inversion	n^3	k^3
Computing velocities	n^2	$k(n-m)$
Computing pressures	n	$n-m$
Computing forces L, D, and S	$3n^2$	$3(n-m)^2$

[a]Note that n is the original number of panels, m is the number of damaged panels (i.e., $m = \mathrm{Dim}(\Gamma_2)$, and k is the number of panels in the vicinity of the damaged section [i.e., $k = \mathrm{Dim}(\Gamma_3)$].

$$\mathbf{F}^{\mathbf{a}} = \frac{\partial \mathbf{f}^{\mathbf{a}}}{\partial \mathbf{x}^{\mathbf{a}}} = \begin{bmatrix} \mathbf{A} \in R^{6\times 6} & \mathbf{B} \in R^{6\times m} \\ \mathbf{0} \in R^{m\times 6} & \mathrm{diag}(\varsigma_i) \in R^{m\times m} \end{bmatrix} \tag{21}$$

The partitioned matrix **A** involves the partial derivatives of force components with respect to the speed (L_V, D_V, and S_V), which can be calculated by numerical differentiation. The force sensitivities to the changes in circulation components (L_Γ, D_Γ, and S_Γ) involved in the partitioned matrix **B** can be evaluated inside the DVLM solver, which reduces the computational load. Two different perturbation models for the differential circulation-strength estimator were formulated. Based on the magnitude of expected changes in the estimated differential circulation strengths, these are termed the heavy- and light-perturbation models.

1. *Heavy-Perturbation Model*

The state vector $\delta\Gamma$ is the perturbation term defined as

$$\Gamma_d = \Gamma_u + \delta\Gamma \tag{22}$$

where $\Gamma_\mathbf{u}$ is the circulation vector for the unimpaired case, and $\Gamma_\mathbf{d}$ is for the impaired case. Note that this formulation attempts to estimate the entire differential circulation-strength vector. To achieve a better filter performance, first-order Markov processes [6] are employed for the differential circulation states. A small leakage constant ζ, which provides fictitious damping to the filter, is introduced to improve the condition of the estimation problem. If ζ is set to zero, $\delta\Gamma$ follows a standard Wiener process.

2. *Light-Perturbation Model*

The second differential approach attempts to determine the changes in the differential circulation-strength vector defined as

$$\Gamma_d = \Gamma_d^{\mathrm{DVLM}} + \delta\Gamma \tag{23}$$

In this case, the circulation-strength vector for the impaired case is calculated using the DVLM, and the perturbation of this circulation-strength vector is estimated using the EKF. This reduces the absolute magnitude of the perturbation by exploiting the DVLM more effectively, possibly leading to a better estimation performance.

This procedure requires the DVLM solver to run at each time step and is computationally more intensive than the heavy-perturbation approach. However, the computational requirements of DVLM approach are modest, enabling its use in the EKF algorithm.

B. Formulation 2: Estimator Based on Parameterized Description of the Damage

The second formulation is based on damage parameterization in which the parameter state represents the size or extent of damage. The filter directly estimates the actual size of the damage using sensor measurements, and the DVLM algorithm provides circulation-strength solutions and the resulting forces on the airframe. This approach has several advantages over the circulation estimation approach given previously.

First, the filter is robust to initial error, and the uncertainty in the initial damage estimate determined from sensors, since the damage size is directly estimated by the filter. Second, the damage parameterization generally involves a much smaller number of parameter states when compared with the number of circulation states. This reduces the number of state variables to be estimated, improving the system's observability and estimator performance.

The major limitation of this damage estimation approach is that the DVLM module has to be run at each time step. Moreover, sufficient accuracy is required for the DVLM solver, since its output is directly used for the subsequent force evaluation without being updated by sensor measurements. To improve the accuracy, the original DVLM solver is modified using the Gauss–Seidel smoothing procedure, which incurs a slight increase in computational cost.

However, various numerical experiments during the present research have revealed that the proposed approach can provide higher accuracy with improved computational efficiency. Figure 6 gives the structure of the estimator. Note that this is a slightly modified version of the estimator given in Fig. 5. The filter employs the sensor measurements in conjunction with the forces computed from the DVLM solver to update the damage parameter state. As stated in the Introduction, it is assumed that the information required

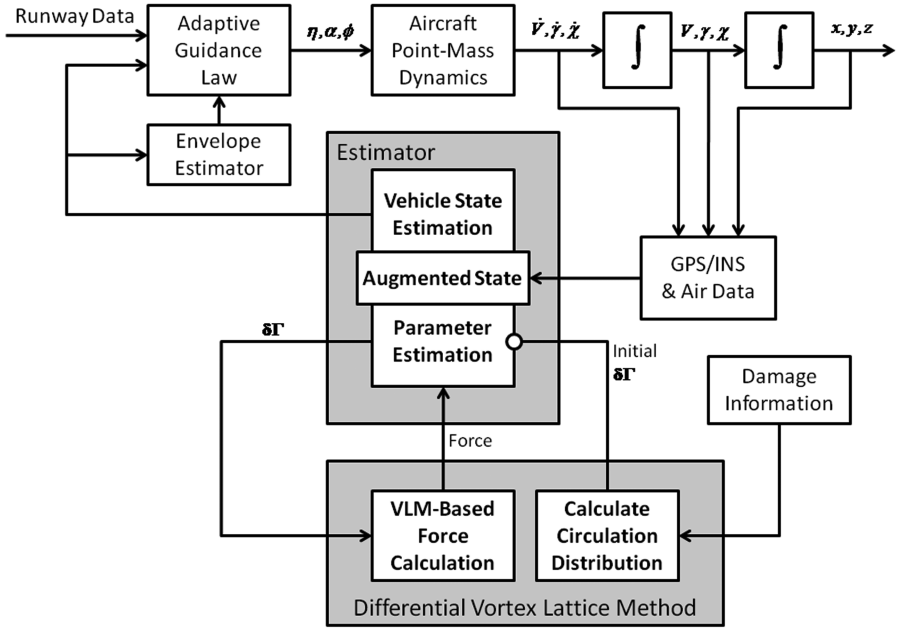

Fig. 5 Filter structure for circulation-strength estimation.

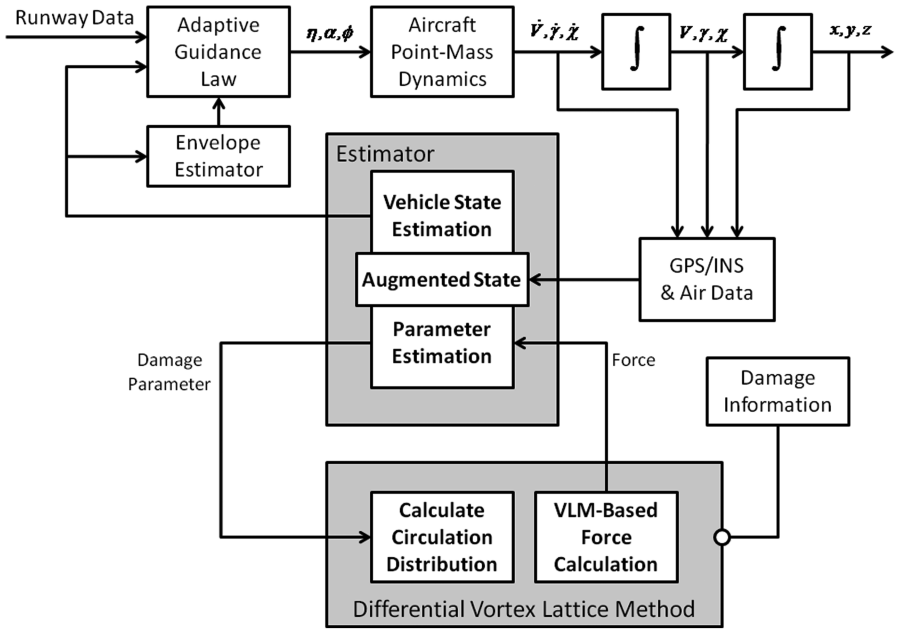

Fig. 6 Filter structure for parameterized-damage estimation.

for parameterizing the damage is available from onboard electro-optical sensors.

The augmented system state for state-parameter estimation can be expressed by

$$\dot{\mathbf{x}}^{\mathbf{a}} = \begin{bmatrix} \dot{V} \\ \dot{\gamma} \\ \dot{\chi} \\ \dot{x} \\ \dot{y} \\ \dot{z} \\ \dot{\theta}_1^d \\ \vdots \end{bmatrix} = \begin{bmatrix} (\eta T - D)/M - g\sin\gamma \\ (L\cos\phi - S\sin\phi)/(MV) - g\cos\gamma/V \\ (L\sin\phi - S\cos\phi)/(MV\cos\gamma) \\ V\cos\gamma\sin\chi \\ V\cos\gamma\cos\chi \\ V\sin\gamma \\ -\zeta_1\theta_1^d \\ \vdots \end{bmatrix} + \mathbf{w}^{\mathbf{a}} \tag{24}$$

Here, θ^d are the damage parameters. The Jacobian matrix for the system dynamics can be represented as

$$\mathbf{F}^{\mathbf{a}} = \frac{\partial \mathbf{f}^{\mathbf{a}}}{\partial \mathbf{x}^{\mathbf{a}}} = \begin{bmatrix} \mathbf{A} = \frac{\partial \mathbf{f}}{\partial \mathbf{x}} \in R^{6\times 6} & \mathbf{f}_{\boldsymbol{\theta}} = \frac{\partial \mathbf{f}}{\partial \boldsymbol{\theta}} \in R^{6\times \mathrm{Dim}(\boldsymbol{\theta})} \\ \mathbf{0} \in R^{\mathrm{Dim}(\boldsymbol{\theta})\times 6} & \mathrm{diag}(\zeta_i) \end{bmatrix} \tag{25}$$

The partitioned Jacobian matrix $\mathbf{f}_{\boldsymbol{\theta}}$ needs to be evaluated numerically, due to the complexity of the relationship between damage parameterization and the system dynamics. In fact, the damage parameterization can be done in various ways. A parameterization scheme using a single-scalar damage parameter is employed in the present research. Specifically, the number of impaired panels, which is a direct measure of the impaired area, is used as a parameter state. Illustrative examples of the parameter numbering schemes depending on damage configurations are shown in Figs. 7 and 8.

V. Simulation Results and Performance Analysis

A series of numerical simulations are set up to evaluate the performance of the state-parameter estimation methods discussed in this section. The full VLM is used for simulating the actual aircraft dynamics, and the DVLM-based EKF formulations are used for online estimation of aircraft states and parameters.

A. Simulation Scenarios

The two following damage configurations are considered for the present simulations. Case 1, wing-tip damage, is shown in Fig. 9 and case 2, hole-in-the-wing damage, is shown in Fig. 10.

Note that the term *damage* in this paper implies the loss of lifting-surface panels on which the circulation strengths are zero. The simulation settings for the filter simulations in this research are as follows. The aircraft weight is 45,941 kgf, the nominal thrust 5791 N, the nominal angle of attack is 6°, the initial speed is 130 kt, and the initial altitude is 3000 m. The process noise covariance matrix is set to $\mathbf{Q} = \mathrm{diag}(0, 0, 0, 0, 0, 0, 1, \ldots, 1)$ and the measurement noise covariance matrix is set to

$$\mathbf{R}_k = \mathrm{diag}(0.12, 0.001752, 0.001752, 1.02, 1.02, 1.02, 1.02, 0.01752, 0.01752)$$

These noise covariance matrices are kept fixed during the simulations.

Note that no environmental disturbance noise for the system states is assumed; however, artificial disturbance is introduced to the parameter states in order to facilitate parameter estimation. The size of artificial disturbance needs to be determined considering the tradeoff between the filter accuracy and convergence speed. The

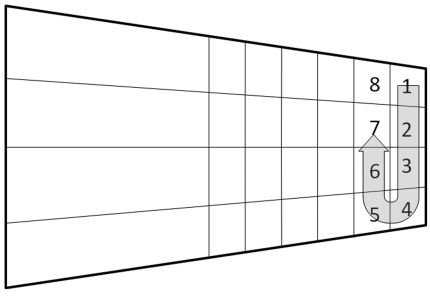

Fig. 7 Tip damage parameterization.

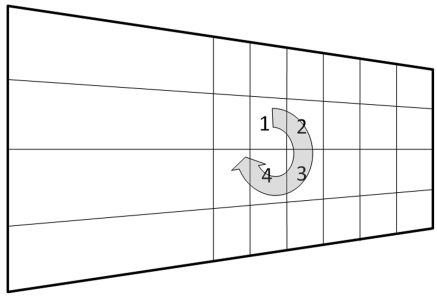

Fig. 8 Hole damage parameterization.

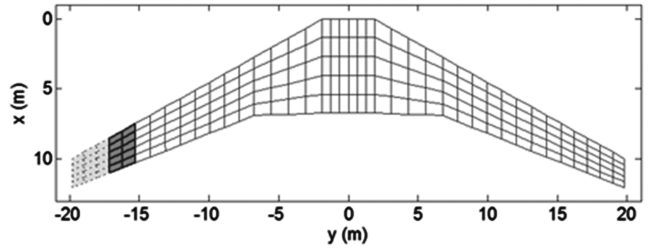

Fig. 9 Damage configuration (case 1): total number of panels is 200, number of impaired panels is 15, and number of panels for DVLM analysis is 10.

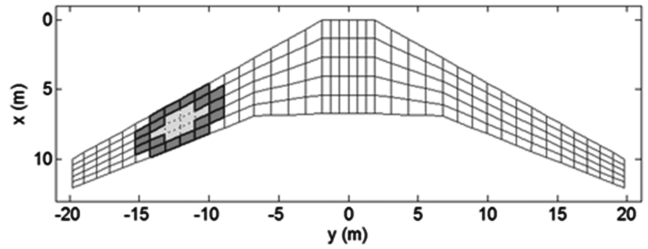

Fig. 10 Damage configuration (case 2): total number of panels is 200, number of impaired panels is 8, and number of panels for DVLM analysis is 18.

measurement noise level also affects the filter performance. In general, the lower that the noise level, the better the filter performance can be expected. However, some special care has to be taken when determining the measurement noise level, since an excessively low noise level may induce numerical instability due to the characteristics of the standard Kalman filter.

B. Information-Enhancing Input Design

The parameter states for modeling the change of aircraft dynamics due to airframe damage are not directly measured, and thus their values have to be indirectly estimated from the aircraft motion sensor measurements. Sometimes these parameter states may be unobservable or indistinguishable from each other, especially when damage profiles are complex or multiple damage clusters exist. The aircraft dynamics in such a situation cannot be expected to be fully observable in terms of the traditional definition of observability in linear systems. However, the nonlinear coupling and interaction between the system dynamics and the measurement equations often make the system observable if appropriate probing actions are employed. For linear systems, observability depends only on the system dynamics and the choice of sensors. That is, once the system dynamics and a sensing configuration are given, the observability is not affected by any external control or trajectory change. However, when nonlinearities are involved in the system, the observability can be affected by the system's state trajectory caused by a specific control input [13,14]. This effect can be exploited to enhance the system observability.

However, designing good and efficient probing inputs involves nonlinear stochastic optimization, which is a challenging topic and remains an open research issue. In the present research, more emphasis is placed on demonstrating the feasibility of the proposed DVLM-based damage estimation algorithm, and relatively simple and common oscillatory probing inputs are employed. That is, sinusoidal inputs with the different frequency and amplitude in angle of attack, angle of sideslip, and bank angle are used as the information-enhancing inputs. The amplitudes of these inputs are determined based on sensitivity analysis, and the excitation frequency and simulation time span are chosen based on the period of the phugoid mode [15]. Figure 11 illustrates the control input histories used to generate the results given in this section.

For the present simulations, the angle of attack starts from the nominal equilibrium value of 6° for the unimpaired aircraft.

C. Simulation Results

Perturbation models in Eqs. (22) and (23) are used in the estimation algorithm for the two damage scenarios. It is assumed here that 15 panels are impaired in the wing-tip damage configuration, and eight panels are impaired in the hole-in-the-wing

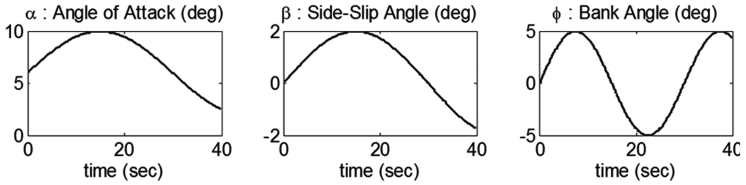

Fig. 11 Aircraft inputs used in the simulation.

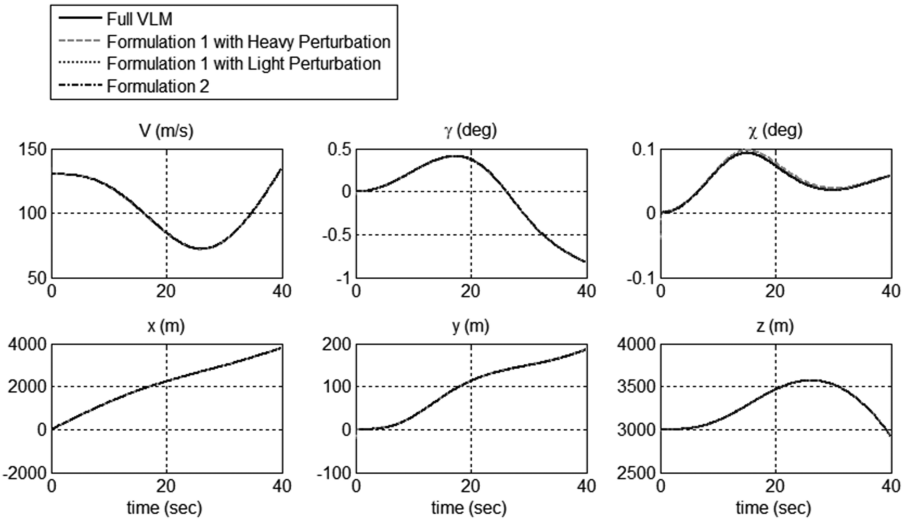

Fig. 12 Aircraft motion states by the full VLM and the DVLM estimators (wing-tip damage).

damage configuration. The dimension of the circulation state vector varies depending on the damage configuration for the filter based on formulation 1. To construct the circulation state vector for this approach, 10 panels are used for the wing-tip damage configuration, and 18 panels are used for the hole-in-the-wing damage configuration.

Figure 12 compares the actual motion state trajectories by the full VLM and the state estimates by the DVLM-based estimators for the wing-tip damage scenario. In Fig. 13, for the same damage scenario, only the motion state estimator errors are plotted for a more explicit quantitative comparison between the three estimators: two for formulation 1 and one for formulation 2. In the figures, the dotted lines and the dashed lines correspond to the DVLM estimators based on formulation 1, and the dashed–dotted lines are the error histories from the parameterized-damage estimator based on formulation 2. Note that the damage is assumed to occur at $t = 0$.

Figures 14 and 15 are for the hole-in-the-wing damage scenario.

All of the proposed formulations show satisfactory performance for the aircraft motion state estimates. In particular, excellent filter performance is observed for formulation 1 with light perturbation and formulation 2, whose estimates almost exactly lie on the actual motion state trajectories (see Figs. 12 and 14). This is mainly because of the availability of direct measurements for all those motion states in the measurement equation shown in Eq. (5).

However, their performance in estimating unmeasured states and resulting aerodynamic forces greatly vary depending on the formulations and perturbation models. The aerodynamic force evaluation results for the wing-tip damage are shown in Figs. 16 and 17, and those for the hole-in-the-wing damage scenarios are shown in Figs. 18 and 19.

Regarding formulation 1, the filter with light perturbation outperforms the heavy-perturbation filter. The performance of the heavy-perturbation model is inadequate. The leakage constant provides artificial system damping and prevents the filter from diverging. However, the filter with heavy perturbation basically lacks numerical stability. This approach estimates the circulation-strength difference due to the damage solely based on the EKF algorithm without using DVLM correction information explicitly, and the filter was found to be incapable of dealing with the substantial nonlinearities in the system. The light-perturbation model, on the other hand, employs smaller corrections, uses more information from the DVLM solver, and shows improved performance considering the system's marginal observability and the minor inaccuracies in the DVLM. In fact, this observation led to the conjecture that using

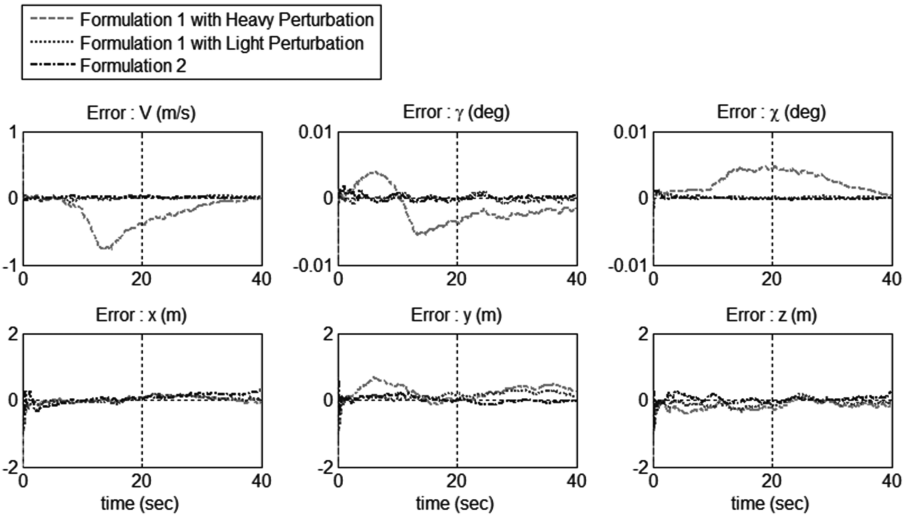

Fig. 13 Errors in the aircraft motion state estimates (wing-tip damage).

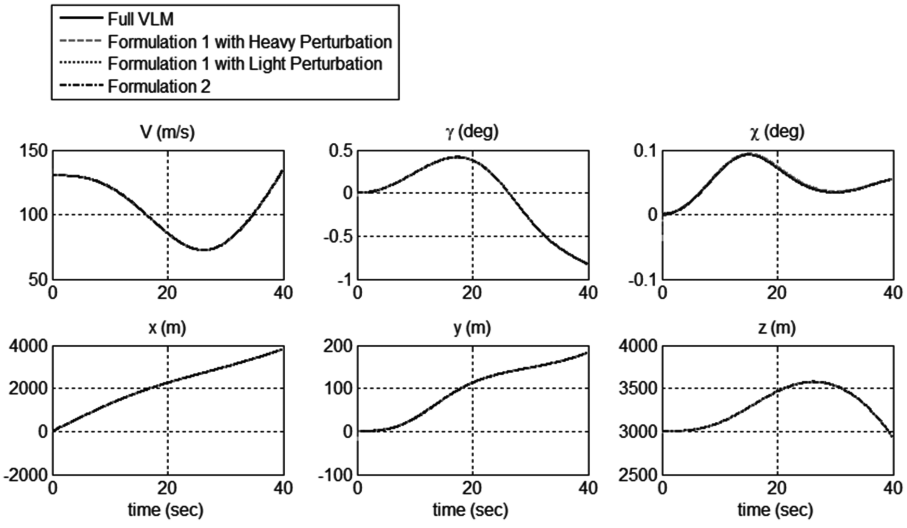

Fig. 14 Aircraft motion states by the full VLM and the DVLM estimators (hole-in-the-wing damage).

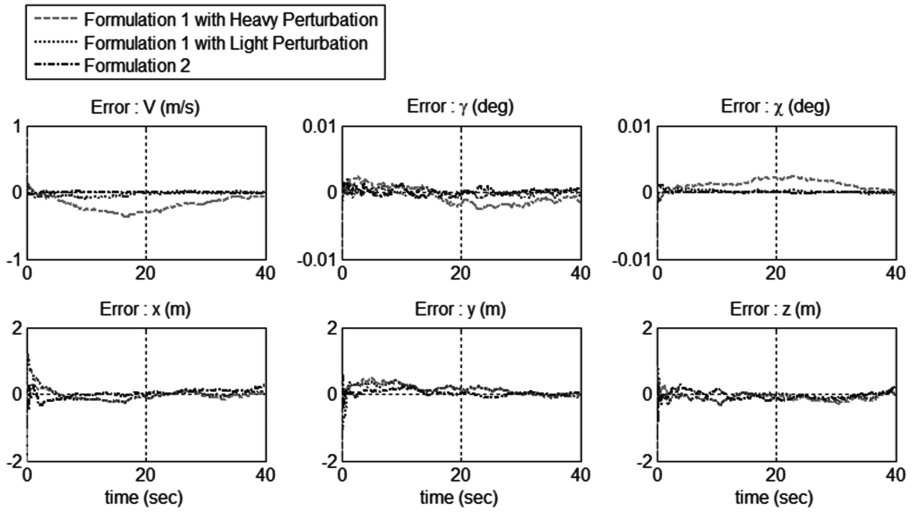

Fig. 15 Errors in the aircraft motion state estimates (hole-in-the-wing damage).

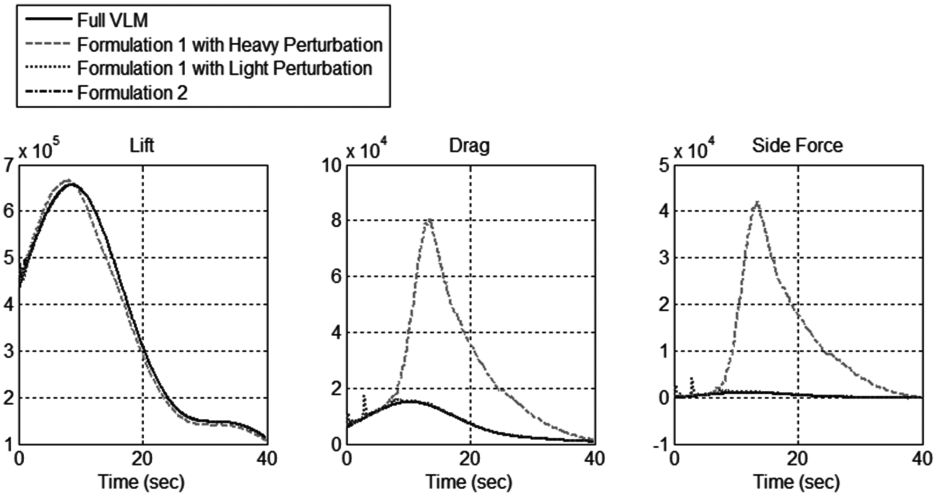

Fig. 16 Aerodynamic forces by the full VLM and the DVLM estimators (wing-tip damage).

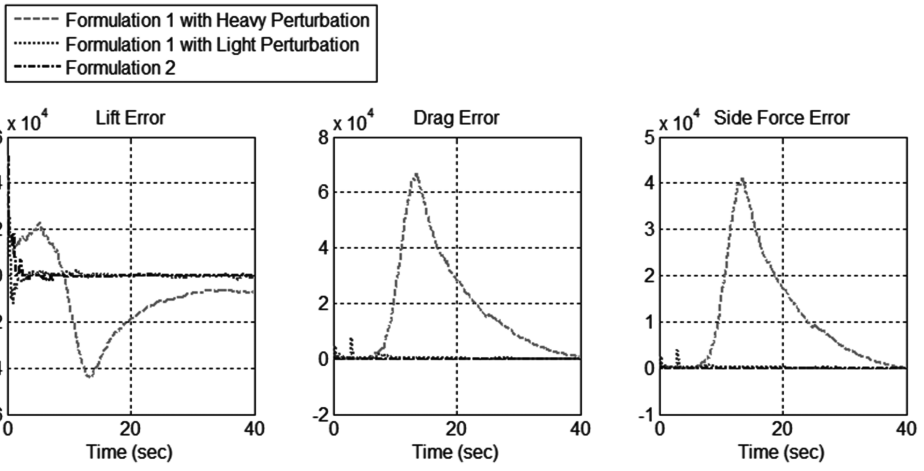

Fig. 17 Errors in the aerodynamic force estimates (wing-tip damage).

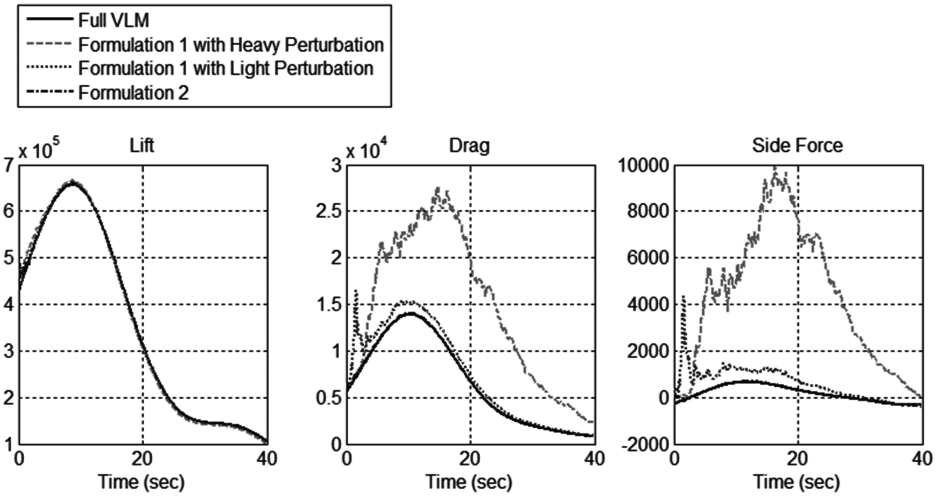

Fig. 18 Aerodynamic forces by the full VLM and the DVLM estimators (hole-in-the-wing damage).

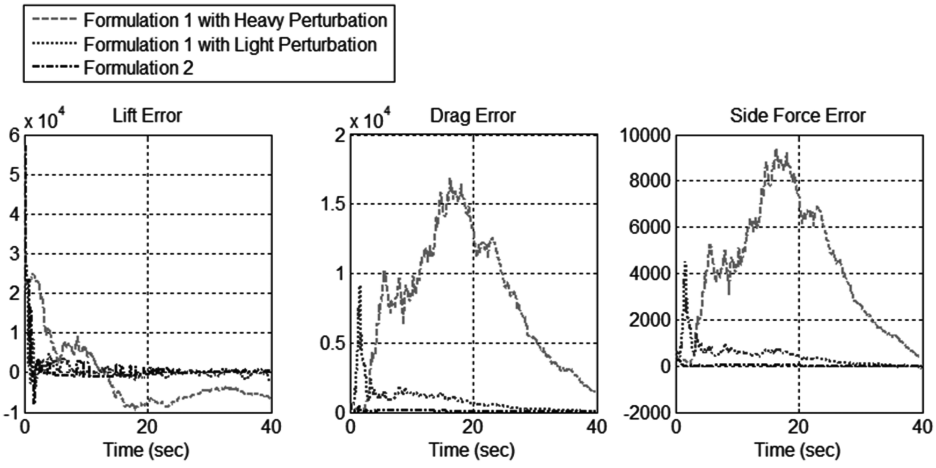

Fig. 19 Errors in the aerodynamic force estimates (hole-in-the-wing damage).

the DVLM as an open-loop solver and focusing on improving the accuracy of inputs to the DVLM solver might provide better overall performance, which resulted in the second formulation with direct damage parameterization.

As can be observed in the above figures, the second formulation provides excellent filter performance. In addition to the accurate estimation of the aircraft states, good force estimation results are obtained. The state estimate for the number of impaired panels for the hole-in-the-wing damage configuration is shown in Fig. 20. Figure 21 compares the associated circulation strengths and the results by the full VLM formulation.

Figure 20 shows that the estimate converges within a few seconds; however, steady-state errors remain. This error is due to the difference between the full VLM and DVLM formulations. The error can be reduced by improving the accuracy and fidelity of the DVLM algorithm.

For the hole-in-the-wing damage, the panels with the identification numbers 153, 157, 158, 159, 162, 163, 164, and 168 are the impaired panels on which circulation strengths are zero, and the adjacent panels are the boundary panels. Some errors and ambiguities are observed near the boundaries of the damage, due to the errors in the estimation of the number of impaired panels and the approximation algorithm by the DVLM algorithm. However, the overall estimation performance appears to be very satisfactory. In particular, it is observed that the circulation-strength prediction errors based on the estimated parameter are quite localized. Another advantage of this formulation is that the filter dimension and its convergence rate are not explicitly dependent on the resolution of the airframe geometric discretization used in formulating the DVLM.

The following observations can be made from the plots in Figs. 12–21:

1) The filter using DVLM formulation 1 with the light-perturbation model and the filter using formulation 2 with the parameterized damage outperform the filter using the DVLM formulation 1 with the heavy perturbation.

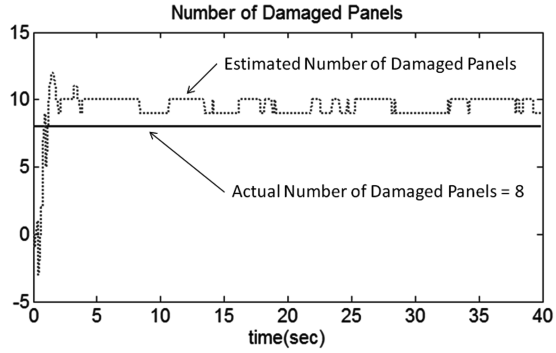

Fig. 20 Estimate of the number of impaired panels (formulation 2, hole-in-the-wing damage).

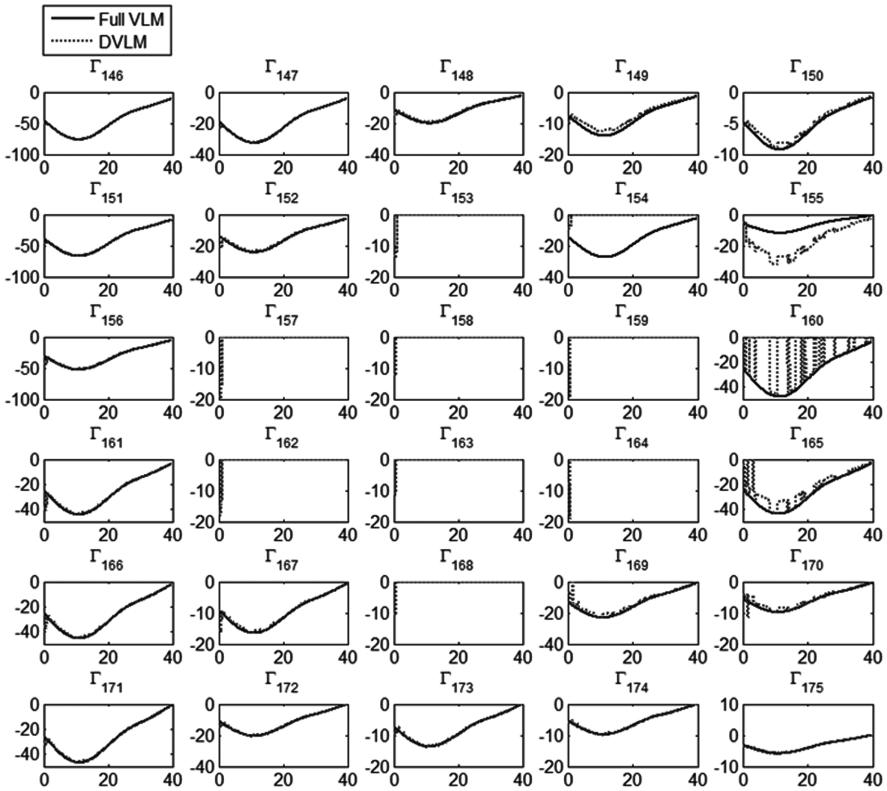

Fig. 21 Circulation vector estimates: VLM vs DVLM + EKF (formulation 2, hole-in-the-wing damage).

Table 3 Performance summary

	Formulation 1		
Filter formulation	Heavy perturbation	Light perturbation	Formulation 2
State-dimension scalability	Poor	Poor	Good
Dependency on DVLM	Low	Moderate	High
Overall computational cost	Low to moderate	Moderate to high	Moderate
Estimation accuracy	Poor	Fair	Good
Filter stability and robustness	Poor	Fair	Good

2) The filter using formulation 2 shows the best force estimation performance among the three proposed approaches, especially during the transient phase.

Table 3 summarizes the performance comparison between the three approaches proposed in this paper.

VI. Conclusions

This paper described extended Kalman filter algorithms based on a differential vortex-lattice method to realize a practical approach for determining the aerodynamic model of an impaired aircraft and to use it as the basis for estimating flight constraints. The present research was motivated by the desirability of relating the impaired-aircraft geometry with its flight dynamics. The central premises involved in the research are that the inner-loop flight control system allows the continued flight of the aircraft, the onboard sensors can provide information about the location and qualitative nature of the damage on the airframe, and the vortex-lattice method can provide sufficiently accurate aerodynamic characterization of the aircraft.

A novel, computationally efficient, algorithm for computing the aerodynamic forces on impaired aircraft, termed the differential vortex-lattice method, was advanced in this paper. This algorithm uses prior knowledge of the aerodynamic model to derive a differential formulation of the well-known vortex-lattice method. It was shown that the algorithm is accurate and can provide significant savings in computational time when compared with the vortex-lattice method. Computationally efficient differential formulations developed in this paper make it possible to rapidly estimate the aerodynamic model of impaired aircraft and to eventually use it for designing safe landing guidance algorithms.

The differential vortex-lattice algorithm was then used as the basis for the design of three extended Kalman filters. Using a point-mass dynamic model, these estimators were shown to be capable of extracting the impaired-aircraft aerodynamic parameters from the motion measurements. Accurate estimation of the aircraft motion and the aerodynamic parameters using the extended Kalman filters was demonstrated in two distinct damage simulations. Numerical simulations were performed to demonstrate and compare the performance of the proposed filtering algorithms. The results confirm that formulation 2, based on the direct damage parameterization, outperforms the other approaches that estimate circulation strengths.

Acknowledgments

This research was supported under NASA contract no. NX08CA50P, with Diana Acosta of NASA Ames Research Center serving as the Technical Monitor. We would like to thank K. Krishnakumar and Nhan Nguyen of NASA for their interest and support of this research.

References

[1] Nguyen, N., Krishnakumar, K., Kaneshige, J., and Nespeca, P., "Dynamics and Adaptive Control for Stability Recovery of Damaged Asymmetric Aircraft," AIAA Guidance, Navigation, and Control Conference, Keystone, CO, AIAA Paper 2006-6049, 2006.

[2] Nguyen, N., Krishnakumar, K., Kaneshige, J., and Nespeca, P., "Flight Dynamics and Hybrid Adaptive Control for Stability Recovery of Damaged Asymmetric Aircraft," *Journal of Guidance, Control, and Dynamics*, Vol. 31, No. 3, 2008, pp. 751–764. doi:10.2514/1.28142

[3] Rysdyk, R. T., and Calise, A. J., "Fault Tolerant Flight Control via Adaptive Neural Network Augmentation," AIAA Guidance, Navigation, and Control Conference, AIAA Paper 98-4483, Boston, 1998.

[4] Kuethe, A. M., and Chow, C-Y., *Foundations of Aerodynamics*, Wiley, New York, 1998.

[5] Morgan, J., *An Introduction to Theoretical and Computational Aerodynamics*, Wiley, New York, 1984, pp. 130–134.

[6] Gelb, A., *Applied Optimal Estimation*, MIT Press, Cambridge, MA, 1989.

[7] Bar-Shalom, Y., Li X. R., and Kirubarajan, T., *Estimation with Applications to Tracking and Navigation*, Wiley, New York, 2001.

[8] Jazwinski, A. H., *Stochastic Processes and Filtering Theory*, Academic Press, New York, 1970.

[9] Astrom, K. J., and Wittenmark, B., *Adaptive Control*, Addison-Wesley, Menlo Park, CA, 1989.

[10] Melin, T., "A Vortex Lattice MATLAB Implementation for Linear Aerodynamic Wing Applications," M.S. Thesis, Dept. of Aeronautics, Royal Inst. of Technology (KTH), Stockholm, 2000.

[11] Magnus, A. E., and Epton, M. A., "PAN AIR-A Computer Program for Predicting Subsonic or Supersonic Linear Potential Flows About Arbitrary Configurations Using A Higher Order Panel Method, Vol. 1: Theory Document (Version 1.0)," NASA CR-3251, 1980.

[12] Miranda, L. R., Elliott, R. D., and Baker, W. M., "A Generalized Vortex Lattice Method for Subsonic and Supersonic Flow Applications," NASA CR-2865, 1977.

[13] Maybeck, P. S., *Stochastic Models, Estimation, and Control*, Vol. 3, Academic Press, New York, 1982, pp. 245–255.

[14] Kim, J., and Rock, S., "Feedback Dual Controller Design and Its Application to Monocular Vision-Based Docking," *Journal of Guidance, Control, and Dynamics*, Vol. 32, No. 4, 2009, pp. 1134–1142. doi:10.2514/1.41957

[15] Blakelock, J. H., *Automatic Control of Aircraft and Missiles*, Wiley, New York, 1991, pp. 50–53.